Geomagnetic Cutoffs for Cosmic-Ray Protons for Seven Energy Intervals between 1.2 and 39 Mev

J. L. FANSELOW[1] AND E. C. STONE

California Institute of Technology, Pasadena, California 91109

The vertical geomagnetic cutoffs for cosmic-ray protons are presented for seven different energy intervals between 1.2 and 39 Mev. These data, representing approximately 160 passes through the cutoff, were taken during 1967 and 1968, between 408- and 912-km altitude, during times of $K_p < 1^+$. These passes provide nearly an order of magnitude more data during geomagnetically quiet times than have been previously reported at even one of these energies. In addition, the energy resolution of the instrument was significantly better than that of previous instruments. With these data, we find that the measured invariant latitudes for the cutoffs are 3° to 5° below previous calculations. We were unable to find any correlation of these observations with any physical phenomenon, including DST or the sun-earth-dipole angle. However, these data do indicate that even during 'quiet' times there are temporal changes in the geomagnetic field that cause the cutoff to fluctuate by 1° to 2°.

The geomagnetic field allows charged cosmic-ray particles to reach the earth over only limited regions, the extent of these regions being determined by the rigidity of the particle. For example, protons with energies of ~10 Mv are able to penetrate to the earth only over the polar caps, whereas those of ~18 Gv may be vertically incident at the surface anywhere. In principle, at least, it is possible to determine these access regions for any given geomagnetic field model and particle rigidity.

In practice, such determinations are made numerically by tracing the trajectories of particles of the given rigidity but opposite charge upward from the point in question. Two such calculations [*Taylor*, 1967; *Smart et al.* 1969], both taking into account the magnetic tail of the earth, come closer to explaining the low-energy particle observations than have previous calculations. Comparison of observations with these two calculations, which would implicitly check the field models employed, was the impetus for the analysis described in this paper.

The experiment reported here is a significant improvement over previous experiments. This improvement resulted from increased energy and angular resolution, time coverage extending for more than a year, nearly uniform local time coverage, and almost an order of magnitude more passes through the cutoff than were previously available for $K_p < 1^+$. For more historical perspective, see the review article by *Hoffman and Sauer* [1968], and the recent experimental paper by *Flindt* [1970].

INSTRUMENTATION

The data presented here were obtained by means of the joint cosmic-ray experiment of the University of Chicago and the California Institute of Technology on the polar orbiting satellite Ogo 4. Apogee altitude for this satellite was 908 km, perigee altitude was 412 km, and orbital inclination was 86°. In normal operation, data were recorded and played back each orbit; telemetry from this experiment (experiment 8) was scheduled for alternate two-day intervals from launch on July 28, 1967, until the second tape recorder failed on January 19, 1969.

Figure 1 provides a schematic cross section of the detector, which was mounted on the spacecraft so as to always point vertically away from the earth. Protons arriving within 30° of vertical and having an energy between 1.2 and 39 Mev were accepted for analysis. Protons outside this 30° angle, or with more than 39 Mev of energy, were rejected by the anticoincidence cup D_3. Primarily because of energy loss in the Mylar window, protons of less than 1.2 Mev failed to deposit enough energy to exceed the discriminator threshold on D_1. Pulse-height analysis (256

[1] Now at Jet Propulsion Laboratory, Pasadena, California 91103.

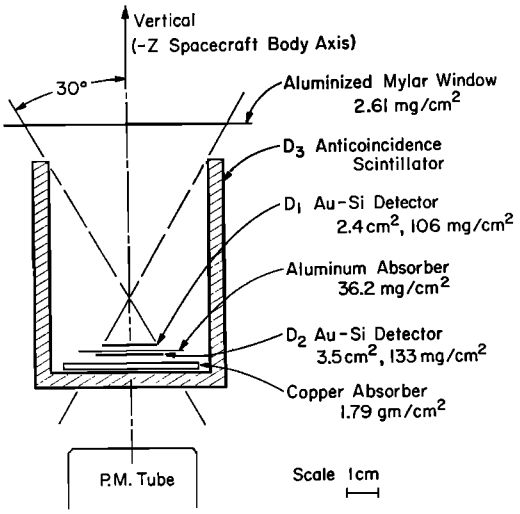

Fig. 1. Schematic cross-sectional view of the vertical particle telescope on Ogo 4. The anticoincidence scintillator is surrounded by 138 mg/cm² of magnesium. D_1 and D_2 both have depletion depths of 56 mg/cm².

channels) of D_1 and a discriminator flag bit on D_2 made it possible to differentiate between protons and higher Z nuclei above about 10 Mev, as can be seen in the response curve shown in Figure 2. Although in principle higher Z nuclei could contaminate the proton response from 1.2 to 10 Mev, such contamination proved to be negligible. Furthermore, while electrons nominally fell below the D_1 threshold, there was a certain probability for electrons to deposit sufficient energy in D_1 to exceed this threshold, either by means of scattering, bremsstrahlung, or pulse pile up. However, both spectral analysis of the 'apparent proton' fluxes and comparison of the $D_2\bar{D}_3$ and the $D_1D_2\bar{D}_3$ count rates indicate that this contamination was less than 15% of the flux in the lowest energy bin for typical flares [*Evans*, 1971]. Laboratory calibrations with an electron beam [*Lupton and Stone*, 1972] and spectral analysis of the 'apparent proton' fluxes show that this source of contamination was completely negligible outside the lowest energy bin. Shown in Figure 2, and also tabulated in Table 1, are the seven subdivisions into which the data were sorted.

DATA ANALYSIS

To locate the boundary between the allowed and forbidden regions ('cosmic-ray cutoff', or 'cutoff' as it will be called hereafter), the data near the cutoff were displayed as shown in Figure 3. In this figure, the abscissa provides universal time, the magnetic equatorial time (MET), and invariant latitude (Λ) of the spacecraft. Invariant latitude was obtained from L in the standard manner:

$$\Lambda = \cos^{-1}(1/L)^{1/2}$$

Magnetic equatorial time of the satellite is defined as the dihedral angle between the dipole meridian passing through the sun and the dipole meridian passing through the intersection of the dipole equator and the line of force on which the satellite is located. Unless otherwise stated, MET and L were calculated in a field consisting of the vector sum of the GSFC 1966 field [*Cain et al.*, 1967] and the Mead external field [*Mead*, 1964]. Use of this particular field model and of MET, rather than the more conventional magnetic local time (MLT), will be justified later in this paper.

The bottom half of Figure 3 consists of a scatter plot of $D1$ pulse height versus time for the two logic groups, $D_1\bar{D}_2\bar{D}_3$ and $D_1D_2\bar{D}_3$. Each individual pulse-height analysis obtained during this particular pass was plotted as a point and was also assigned to one of the energy bins, as is indicated by the scale divisions on the ordinate (refer to Table 1 for the characteristics of these bins). Cumulative counts in each of these bins were also plotted in the upper half of the figure.

The cutoff for a given bin was defined as that latitude at which the rate in that bin was one-half the polar rate (i.e., where the slope of the corresponding cumulative rate plot was one-half its maximum). In practice, because of the sharpness of the cutoff, this particular definition was not at all critical to the results. As an illustration, on the cumulative plot of each bin in Figure 3 an arrow marks the place where the cutoff was declared to occur. Usually this demarcation could be located at a rather unambiguous change in slope. However, the behavior of bins 1 and 4 is more complex. The initial rise in bin 1 resulted from the 15 electrons counted during passage through the outer trapping zone ($65.0° < \Lambda < 68.5°$) and was therefore ignored. In bin 4, particles seem to be arriving at latitudes well below the cutoff of 71.5°. However, these are most likely contamination from particles in the approximate energy range from 8

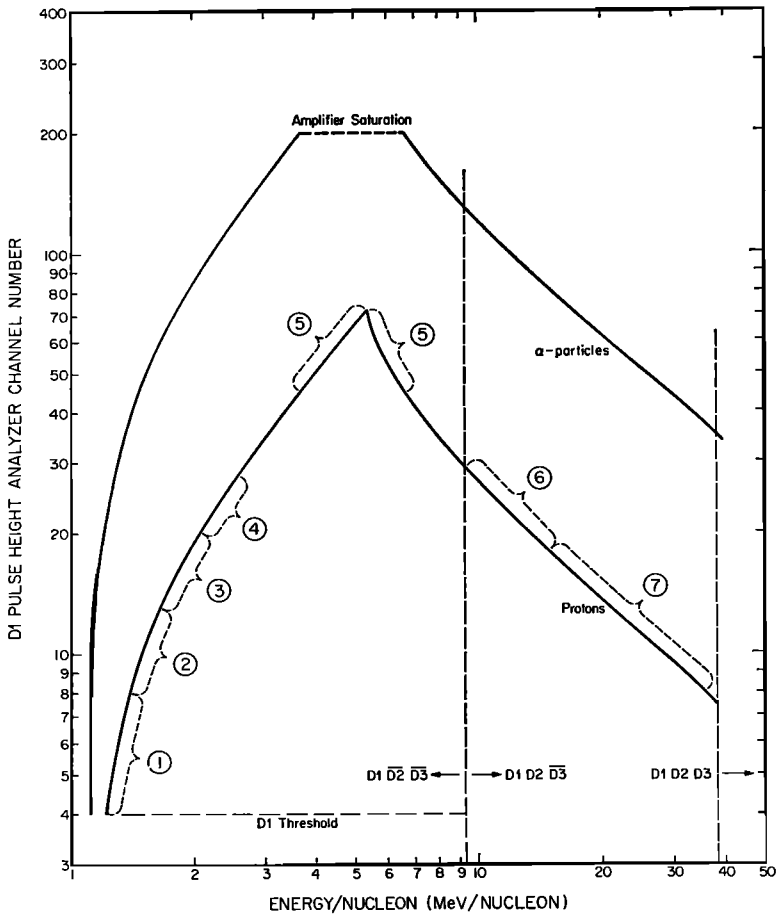

Fig. 2. Calibrated channel number versus threshold energy response of the $D1$ pulse-height analyzer for protons and α particles. The numbered brackets show the energy bins into which the analyzed protons were classified.

to 9.3 Mev. The resolution function of $D1$ in this range is nearly Gaussian (FWHM 20%), and thus there is a small probability that these particles will have energy losses corresponding to bin 4. This distribution is due primarily to fluctuations in energy loss in $D1$, and to spatial variations in the depletion depth of that detector.

In the scatter plot of Figure 3, there is also a hint of spatial structure of the flux at and above the cutoff. In some orbits, this was much more pronounced than it is here, and occasionally it caused some difficulty in the placement of the cutoff. Structure near the cutoff has also been observed even more clearly by *Imhof et al.* [1971]. We acknowledge its presence, but feel that it has not been a significant problem in our final definition of the cutoff. Were we in doubt for a particular pass, we excluded either the involved energy bins or the entire pass.

For the higher-energy bins, the major limitation to the precision with which the cutoff could be determined was statistical. Though we selected only passes in which the flux of protons between 1.2 and 39 Mev was greater than 1 proton cm^{-2} $ster^{-1}$ sec^{-1}, the higher-energy bins often had so low a rate that statistical fluctuations led to imprecise determination of the cutoff.

Because the readout rate of the instrument was limited to 3.47 events/sec, it was possible in certain special cases for the saturation of this readout rate to be confused with the cutoff. We have considered this problem in detail, and find

TABLE 1. Characteristics of the Energy Subdivisions

Bin	Channel	Incident Proton Threshold		Eff. Energy and Rigidity for $dJ/dE = J_0E^{-3}$ Energy Spectrum	
		Mev	Mv	Mev	Mv
$D_1\bar{D}_2\bar{D}_3$					
1	4–7	1.21–1.36	47.7–50.5	1.28	49.0
2	8–12	1.36–1.63	50.5–55.3	1.49	52.9
3	13–19	1.63–2.05	55.3–62.0	1.82	58.5
4	20–27	2.05–2.57	62.0–69.5	2.29	65.6
*	28–44	2.57–3.65	69.5–82.8	3.05	75.7
		6.73–9.3†	113. –132.	7.88	122.
5	45–72	3.65–6.73	82.8–113.	4.88	95.8
$D_1D_2\bar{D}_3$					
6	18–29	9.3†–16.4	132. –176.	12.2	152.
7	8–17	16.4–38.6	176. –272.	24.4	215.

* Because of double-valued range, this channel interval was neither assigned a bin number nor was it utilized in further analysis.

† Determined by threshold of D_2 discriminator, not by pulse-height analyzer.

that in the absence of rate information in all bins it would not have been possible to eliminate readout saturation as a problem in a specific bin. However, we did have the apparent rates in all bins; furthermore, we had rate information for D_1, D_2, and $D_1D_2\bar{D}_3$. Thus we knew the equivalent of the 'normalization' constant as a function of time for the probability that an event in a given bin would be selected for readout. In the vast majority of the passes, such information allowed us to obtain the actual geomagnetic cutoff. However, occasionally these saturation effects could not be unambiguously eliminated, and these affected data points were excluded from further analysis.

For each pass satisfying the above criteria, a cutoff time (UT) for as many as seven different energy bins was obtained. Interpolation of attitude and orbit information to this time provided each cutoff in each energy bin with an array of information representing the position and orientation of the spacecraft at that cutoff. These arrays were used in subsequent analysis. As an example, for a given time, satellite latitude, longitude, and height, we could then calculate the invariant latitude, MET, or the angle of the magnetic field relative to the instrument, using different geomagnetic field models. Similarly, we could obtain the dipole orientation relative to the sun-earth line.

We directed all our further efforts with these data toward finding a means of organizing them better. Since we wish to compare our data with trajectory calculations made in a static field, the data in the arrays described above were the result of passes initially selected for having $K_p < 1^+$. Figure 4 displays these data for 1.8 Mev. In this figure, and in subsequent figures similar to it, each point represents the cutoff position for a single pass. Unfortunately, for this particular satellite and epoch, such a requirement on K_p resulted in a scarcity of data between 1300 and 1500 MET.

In order to determine whether the scatter in the data arose from inaccurate A-MET mapping, different field models were used for the mapping. However, with the data set selected only on the basis of $K_p < 1^+$, little reduction in scatter was achieved, indicating that other sources of cutoff variation dominated. The scatter was significantly reduced, however, by restricting the data to those passes that met the following two criteria: (1) The pass was preceded by at least 6 hours of constant, known sector direction; and (2) $K_p \leq 2^-$ for at least 6 hours before and after the observation.

Such criteria, with the limited data sample we have, should be interpreted only as representing a correlation between these parameters and the unknown physical processes that affect the cutoff. Although the application of these criteria to a larger data set is necessary to

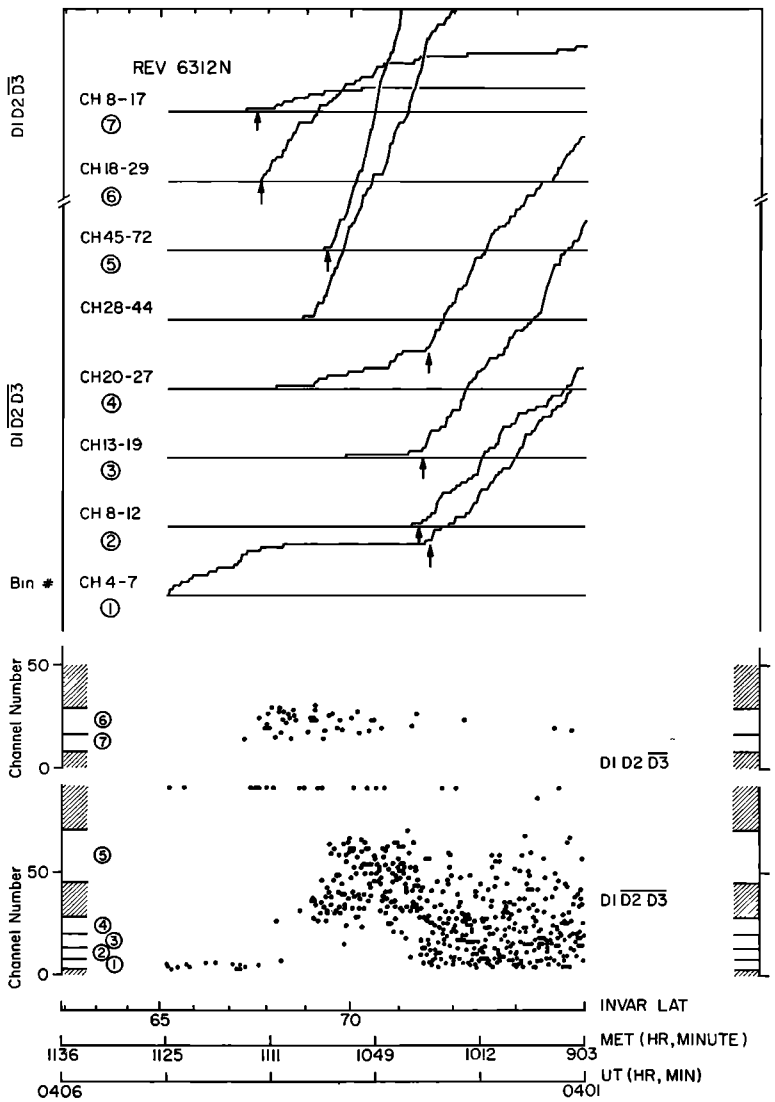

Fig. 3. Pulse-height-analyzer and satellite-position data for the cutoff region on orbit 6312 north. Each analyzed event read out by the spacecraft is plotted as a point corresponding to the appropriate channel number, logic group, and time of occurrence. The curves in the upper part represent cumulative counts for their respective bins. The numbers in circles are the bin numbers, the same as those shown on Figure 2 and in Table 1. The cutoff latitude is indicated by an arrow.

determine their general validity, their application to the present data did produce a subset that demonstrated a dependence on the magnetic field model, as was expected.

Figure 5 represents samples of various mappings used on this subset of 160 passes. In each of the parts of Figure 5, invariant latitude of the cutoff for 1.8-Mev protons is the ordinate, and local time the abscissa. Parts *d* and *e* of this figure display the best organization. For the model with a tail field [*Williams and Mead*, 1965], variation of the relevant parameters had some effect, but no model improved the quality of the mapping over that achieved by the combined GSFC 1966 internal and the Mead external field. Therefore, we chose this geomag-

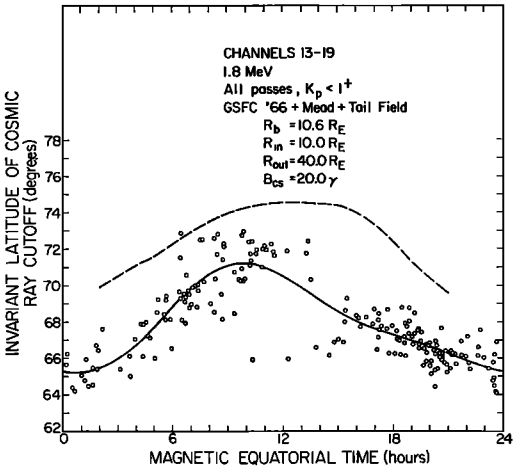

Fig. 4. Invariant latitude of the cosmic-ray cutoff versus magnetic equatorial time for 1.82 Mev. Each point is a single pass during a time when $K_p < 1^+$. The field model used to obtain Λ and MET is the vector sum of the Goddard 1966 internal field [*Cain et al.*, 1967], the Mead external field [*Mead*, 1964], and the Williams-Mead tail field [*Williams and Mead*, 1965]. The dashed curve represents the cutoff calculated by *Smart et al.* [1969], whereas the solid curve is a curve fit to the data.

netic field model to map our results, rather than using the more complicated models involving tail fields.

The slight improvement from using MET rather than MLT is presumably because the data are better organized by the local time at the equatorial crossing of the field line rather than by the local time at the foot of the field line, where the geomagnetic field has significant azimuthal variations due to higher-order terms in the field expansion. With only an internal field, MET and MLT differ by less than 1 hour at $\Lambda \sim 70°$, with a rms difference of $\sim$0.5 hour. The Mead external field and the Williams-Mead tail field produce an additional systematic difference of approximately -0.5 hour at 0600 MLT and $+0.5$ hour at 1800 MLT and less at other times.

All further efforts toward organization did not improve on that represented in Figure 5*d* and 5*e*, despite the fact that for any given pass, particularly on the nightside, the cutoff could be determined to within a few tenths of a degree invariant latitude. Moreover, for multiple passes within a few hours of each other, the cutoffs often seemed to lie along a mean line in Λ-MET space, their scatter being typically 0.2° latitude. However, if we combined many passes together as we have done in Figure 5, the spread of the data was $\sim$1°–2°.

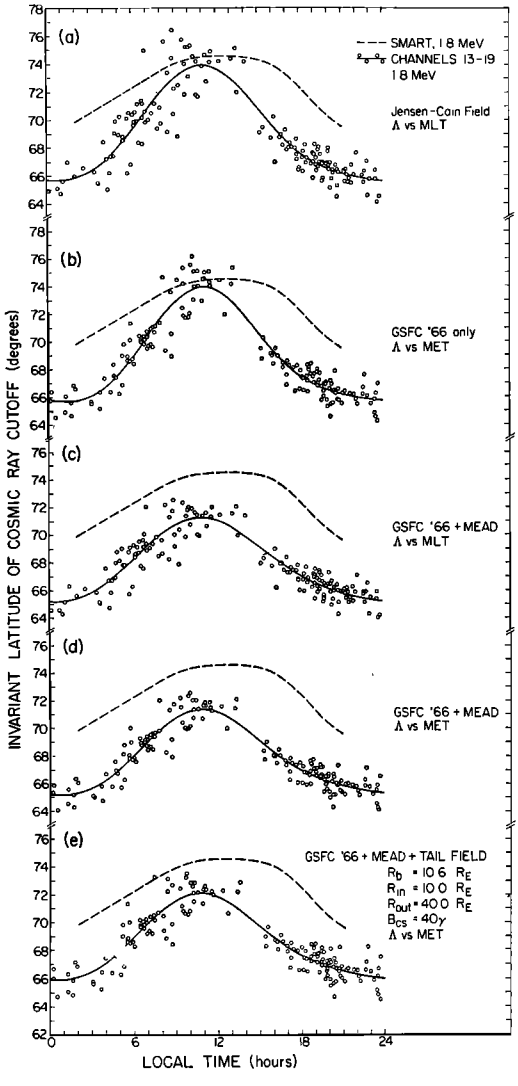

Fig. 5. Invariant latitude Λ of the cosmic-ray cutoff versus local time for energy group 3. The same data are plotted in each of the five sections. The only changes between sections are changes in the definition of local time and the field model in which invariant latitude and local time are calculated. The cutoffs calculated by *Smart et al.* [1969] are shown by the dashed lines. No attempt has been made to map their results to the field and local time under consideration. The solid curves are fits to the data.

Attempts to treat this spreading as fluctuations about some mean curve in Λ-MET space yielded no significant correlation with the satellite height or magnetic field. Thus we conclude that these variations were not due to variations in shadowing by the earth, mirroring effects at different values of the magnetic field, or variations in the fraction of the detector geometry available to particles of a given pitch angle.

One other possible explanation considered was that somehow these variations were introduced by our definition of the cutoff. As a check, we considered only those passes in which there were no ambiguous cutoffs due to flux structure near the cutoff, and further, only those passes where the statistics were also definitely good enough to locate the cutoff to well within 0.2°. Even this did not produce a significant change in the spread.

Similarly, with the field model used, we could obtain no significant correlation between the deviations from a mean Λ-MET curve and (1) universal time, (2) dipole longitude, or (3) the angle between the sun-earth line and the dipole axis. From 3 we conclude that the wobble of the dipole relative to the solar-wind velocity direction causes residual variations of less than 0.5° when averaged over several hours of local time, which is consistent with the calculations of *Burch* [1971]. From 1 and 2 we infer that the field model is generally correct. Although we cannot unequivocally rule out the possibility that the scatter in the data is still a mapping effect, addition of the next most obvious improvement to the field model, a current sheet in the tail, did not help. Altering the higher-order coefficients in the Mead external field by 50% also produced no significant change. Therefore, we find it unlikely that this scatter is caused by mapping problems of a static field.

In a preliminary study, we did find that the cutoff was related to K_p, as have other investigators [*Paulikas et al.*, 1970; *Imhof et al.*, 1971]. During times of high K_p, the cutoff was often, though not always, lower than our average quiet-time value by as much as 2° or 3°. That was the reason for our initial restriction to data taken during times when $K_p < 1^+$. However, with this restriction, we could obtain no further significant correlation between K_p and cutoff latitude. Similarly, we were unable to correlate our quiet-time cutoff data with DST or with the time derivative of DST, at least not in a simple manner. This remained the case even though we introduced relative time shifts of up to 15 hours in either direction.

As a means of summarizing our data, we have fit either one of two functional forms to the data in Λ-MET space. For energies less than 10 Mev, this function was

$$\Lambda = A + B\cos(\mathrm{MET}\cdot\pi/12) + C\sin(\mathrm{MET}\cdot\pi/12) + D\cos(\mathrm{MET}\cdot\pi/6) + E\sin(\mathrm{MET}\cdot\pi/6) \quad (1)$$

For energies above 10 Mev, we fit the shape calculated by *Smart et al.* [1969] minus a constant:

$$\Lambda = \Lambda_{\mathrm{Smart}} - A \quad (2)$$

The values for the parameters are given in Table 2. Use of two frequencies in MET space

TABLE 2. Parameters for the Functions Fitted to the Data

Effective Energy, Mev	Function Fit to Data	Constant, deg				
		A	B	C	D	E
1.28	1	68.23	−3.12	0.71	0.17	−0.55
1.49	1	68.00	−3.01	0.61	0.25	−0.48
1.82	1	67.84	−2.95	0.57	0.34	−0.47
2.29	1	67.53	−2.77	0.65	0.36	−0.46
4.88	1	66.77	−2.30	0.28	0.60	−0.30
12.2	2	3.03				
24.4	2	2.38				

Function 1: $\Lambda = A + B\cos(\mathrm{MET}\cdot\pi/12) + C\sin(\mathrm{MET}\cdot\pi/12) + D\cos(\mathrm{MET}\cdot\pi/6) + E\sin(\mathrm{MET}\cdot\pi/6)$.

Function 2: Λ = curve of *Smart et al.* [1969] minus A.

provided a better fit than did one. However, going to higher harmonics in MET provided no significant improvement. Above 10 Mev the organization of the data was too poor to justify anything more complex than merely shifting the *Smart et al.* [1969] curves.

DISCUSSION

From these data we have reached the following two conclusions: first, the observed cutoffs lie 3°–5° below the theoretical values, suggesting that the field model or trajectory calculations need revision; second, even during 'undisturbed' times, there are temporal variations in the field that are capable of producing changes in the cutoff of up to about 2°. We were unable to find any phenomenon that correlated with these temporal variations.

Figure 6 displays the final form of the data and provides a comparison of the observations with the numerical calculations. For the sake of clarity, we have not shown data from other experiments. However, we want to mention particularly the results of *Imhof et al.* [1971]. Their data for 2-Mev proton cutoffs extrapolated to $K_p = 0$ agree quite well with ours. As for the models, Taylor's is in best agreement on the nightside, whereas the calculations of *Smart et al.* [1969] give a shape for the cutoff in Λ-MET space that more closely approximates the one observed. Both calculations predict cutoffs at considerably higher latitudes than that observed both in this experiment and earlier work [*Stone*, 1964; *Quenby*, 1969; *Flindt*, 1970; *McDiarmid et al.*, 1971; *Imhof et al.*, 1971; and *Masley et al.*, 1971].

Such discrepancies have been attributed to some sort of diffusion of the particles inward across L shells by *Lanzerotti* [1968], *Paulikas and Blake* [1969], *Williams and Bostrom* [1969],

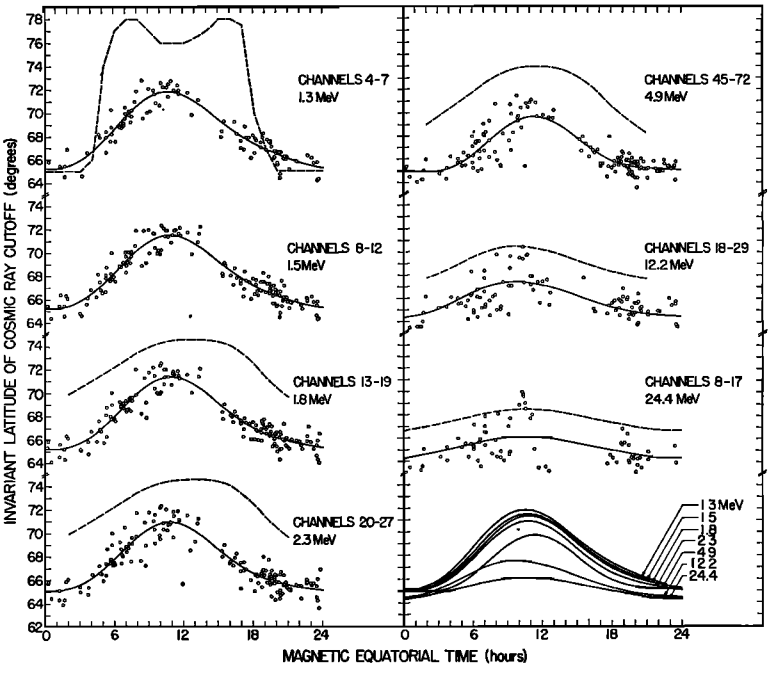

Fig. 6. Invariant latitude Λ of the cosmic-ray cutoff versus MET for all energy bins. Both Λ and MET are calculated in a field that is the vector sum of the Goddard 1966 internal field and the Mead external field. The dashed curves represent the calculations of *Smart et al.* [1969], except for the upper left section, where the dashed curve is from the Taylor model for 1.2-Mev protons [*Taylor*, 1967]. The solid curves are fit to the data as explained in the text, and each point represents a single pass. Solid data symbols represent points excluded from this fit. The lower right-hand section of this figure summarizes the solid curves for the various energies. Note that the two different functions fit to the data give the appearance of a cutoff inversion at ~0400. This is not real.

Paulikas et al. [1970], *Quenby* [1969], and *Imhof et al.* [1971]. *Quenby* [1969] estimated the magnitude of this inward diffusion and concluded that it was consistent with the data available then.

However, net diffusive transport implies a gradient, and thus, if this mechanism is to explain the discrepancy, we should observe a gradually decreasing flux as the satellite proceeds to latitudes below the predicted cutoffs. This we do not see, nor do *Imhof et al.* [1971]. What we do observe is a nearly uniform flux for several degrees below the predicted value, and then a cutoff that takes place in much less than 1°. Our typical cutoff widths of 0.2° are actually commensurate with the proton gyroradius at the surface of the earth for these energies.

It should also be pointed out that in no other region in the vicinity of the earth is the low-energy proton flux any greater than it is in this region of discrepancy, either inside [*Evans*, 1971; *Paulikas et al.*, 1970; *Blake et al.*, 1968; *Williams and Bostrom*, 1969; *McDiarmid and Burrows*, 1969], or outside [*Krimigis et al.*, 1969; *Van Allen et al.*, 1971] the magnetosphere. This, too, is hard to reconcile with simple diffusion as an explanation.

Another discrepancy with the predictions is that our four low-energy intervals have a maximum cutoff latitude at 1100 hours MET, whereas for the corresponding energy in *Smart et al.* [1969] these maximums occur near 1300 local time. Furthermore, between 1800 and 2400 MET our observations show less of a dependence on local time than do their calculations and extrapolations. Neither mapping our results in local time rather than MET, nor using a tail field, significantly alters any of these discrepancies. We feel, therefore, that the predictions need refining.

Using a more realistic inner boundary for the tail, one that more closely followed an L shell rather than a straight line, might conceivably help. It may also be necessary to modify the dayside field. A maximum cutoff latitude at 1100 MET is suggestively similar to the symmetry plane observed at about 1000 local time in studies of trapped and precipitating particles. One possible origin for this effect in the behavior of dayside aurora is discussed by *Forbes and Speiser* [1971].

Our second conclusion is that, although there are significant temporal changes in the field over a 24-hour period, the changes are monotonic and smooth for periods of hours. Evidence for this is that often for a period of a few hours multiple passes would display a scatter of about 0.2° about a mean curve in Λ-MET space.

Figure 7 provides further support for the interpretation that the cutoff fluctuations are not measurement inaccuracies, but are temporal variations occurring simultaneously for all low-energy intervals. The lower part of this figure presents the same data shown in Figure 6, except that the invariant latitude for each pass has been altered before plotting. This alteration consisted of subtracting from the measured cutoff latitude the deviation of the corresponding 1.8-Mev cutoff from the mean curve for 1.8-Mev protons. Passes for which there was no 1.8-Mev cutoff observed were not included. In contrast, the upper part reproduces the unaltered 2.3-Mev data from Figure 6. Similar adjustments of the cutoffs for energies below 2.6 Mev also result in considerably reduced

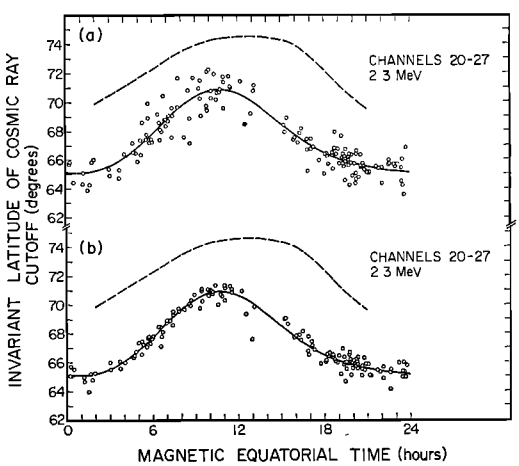

Fig. 7. Data in this figure are for the 2.3-Mev cutoffs. The upper part is the same as the 2.3-Mev section in Figure 6, whereas the lower part represents a subset of the data in the lower half. In this subset, the invariant latitude for each pass was altered before plotting by subtracting a quantity equal to the difference between the 1.8-Mev cutoff latitude observed in that pass and the fitted curve for the 1.8-Mev cutoffs. If no corresponding 1.8-Mev point was available, the pass was not plotted. The dashed curves represent the calculations of *Smart et al.* [1969].

scatter, whereas above that energy the reduction is not nearly so marked, primarily because of the statistical limitations of the lower fluxes. Thus, at least for energies below 2.6 Mev, the time variations in the cutoff latitudes are nearly identical.

Figure 7 may also indicate the limiting precision with which the cutoffs are determined. Only 27 of 138 passes shown lie more than 0.3° from the mean curve in the lower half of the figure.

Large changes in the cutoff may be produced by changes in the current sheet [*Gall et al.*, 1968]. Because the region at the inner edge of the current sheet is critical in determining the position of the cutoff (Gall, private communication, 1970), it may well be that changes in the field model or in the trajectory calculations in this region alone would significantly lower the numerical determinations of the cutoff. If this indeed is the case, then small temporal variations in the configuration there are likely to be responsible for the scatter in our cutoff determination.

Since changes in DST have been attributed to changes in the ring currents, and since we could not correlate DST with our data, we feel that whatever is causing these fluctuations resides outside the ring currents, further motivation for seeking the source of these variations in the tail current sheet. However, since the wobble of the dipole had so little effect, we further expect that this region is close enough to the earth so as to track very closely with the dipole orientation.

SUMMARY

The cutoffs for vertically incident cosmic-ray protons with energies between 1.2 and 39 Mev have a dependence on invariant latitude, local time, and energy similar to that numerically calculated by *Smart et al.* [1969], except that the observations lie generally 3°–5° lower in latitude. We conclude that both this difference, and other features of the data, indicate that either the field model used by *Smart et al.* [1969] or the trajectory calculations need refining, particularly near the last closed field lines on the nightside. The discrepancy is not attributed to radial diffusion. Furthermore, much of the scatter in the data, particularly at midnight local time and low energies, is attributed to slow changes in the field with periods between a few hours and a day. We conclude that the source of these temporal variations lies relatively close to the earth, but beyond the ring currents.

Acknowledgments. We gratefully acknowledge the collaboration and support of Drs. J. A. Simpson and C. Y. Fan during various stages of this joint program of the University of Chicago and California Institute of Technology. The instrument was constructed by the Laboratory for Astrophysics and Space Research of the University of Chicago. We would also like to thank Dr. L. C. Evans and Mr. J. Brown for their helpful suggestions and for some of the subroutines used in the analysis.

One of us (E.C.S.) was an Alfred P. Sloan research fellow during this work.

Funding for the instrument and this analysis came from the National Aeronautics and Space Administration under contract NAS5-3095 and grants NGL 05-002-007 and NGR 05-002-160.

* * *

The Editor wishes to thank H. Sauer and D. F. Smart for their assistance in evaluating this paper.

REFERENCES

Blake, J. B., G. A. Paulikas, and S. C. Freden, Latitude-intensity structure and pitch-angle distributions of low-energy solar cosmic rays at low altitude, *J. Geophys. Res.*, *73*, 4927, 1968.

Burch, J. L., The angle dependence of 10-Mev proton cutoff latitudes, *Rep. X-646-71-344*, Goddard Space Flight Center, Greenbelt, Maryland, 1971.

Cain, J. C., S. J. Hendricks, R. A. Langel, and W. V. Hudson, A proposed model for the international geomagnetic reference field, 1965, *J. Geomagn. Geoelec.*, *19*, 335, 1967.

Evans, L. C., Magnetospheric access of solar particles and the configuration of the distant geomagnetic field, Ph.D. thesis, Calif. Inst. of Technol., Pasadena, 1971.

Flindt, H. R., Local time dependence of geomagnetic cutoffs for solar protons, $0.52 \leq E_p \leq 4$ Mev, *J. Geophys. Res.*, *75*, 39, 1970.

Forbes, T. G., and T. W. Speiser, Mathematical models of the open magnetosphere: Application to dayside auroras, *J. Geophys. Res.*, *76*, 7542, 1971.

Gall, R., J. Jimenez, and L. Camacho, Arrival of low-energy cosmic rays via the magnetospheric tail, *J. Geophys. Res.*, *73*, 1593, 1968.

Hoffman, D. J., and H. H. Sauer, Magnetospheric cosmic-ray cutoffs and their variations, *Space Sci. Rev.*, *8*, 750, 1968.

Imhof, W. L., J. B. Reagan, and E. E. Gaines, Solar particle cutoffs as observed at low altitudes, *J. Geophys. Res.*, *76*, 4276, 1971.

Krimigis, S. M., J. A. Van Allen, and T. P. Arm-

strong, Solar particle observations inside the magnetosphere during the 7 July 1966 proton flare event, *Ann. IQSY, 3,* 395, 1969.

Lanzerotti, L. J., Penetration of solar protons and alphas to the geomagnetic equator, *Phys. Rev. Lett., 21,* 929, 1968.

Lupton, J. E., and E. C. Stone, Electron scattering effects in typical cosmic ray telescopes, *IEEE Trans. Nucl. Sci., NS-19,* 562, 1972.

Masley, A. J., W. P. Olson, and K. A. Pfitzer, Calculation of charged particle entry into polar region, paper presented at the Twelfth International Conference on Cosmic Rays, Hobart, Tasmania, Australia, August 1971.

McDiarmid, I. B., and J. R. Burrows, Relation of solar proton latitude profiles to outer radiation zone electron measurements, *J. Geophys. Res., 74,* 6239, 1969.

McDiarmid, I. B., J. R. Burrows, and M. D. Wilson, Structure observed in solar particle latitude profiles and its dependence on rigidity, *J. Geophys. Res., 76,* 227, 1971.

Mead, G. D., Deformation of the geomagnetic field by the solar wind, *J. Geophys. Res., 69,* 1181, 1964.

Paulikas, G. A., and J. B. Blake, Penetration of solar protons to synchronous altitude, *J. Geophys. Res., 74,* 2161, 1969.

Paulikas, G. A., J. B. Blake, and A. L. Vampola, Solar particle observations over the polar caps, in *Particles and Fields in the Magnetosphere,* edited by B. M. McCormac, p. 141, D. Reidel, Dordrecht, Netherlands, 1970.

Quenby, J. J., The entry of solar protons into the geomagnetic field during the event of June 9, 1968, *Acta Phys. Suppl., 2,* 475, 1969.

Smart, D. F., M. A. Shea, and R. Gall, The daily variation of trajectory-derived high latitude cutoff rigidities in a model magnetosphere, *J. Geophys. Res., 74,* 4731, 1969.

Stone, E. C., Local time dependence of non-Störmer cutoff for 1.5 Mev protons in quiet geomagnetic field, *J. Geophys. Res., 69,* 3577, 1964.

Taylor, H. E., Latitude local-time dependence of low energy cosmic-ray cutoffs in a realistic geomagnetic field, *J. Geophys. Res., 72,* 4467, 1967.

Van Allen, J. A., J. F. Fennel, and N. F. Ness, Asymmetric access of energetic solar protons to the earth's north and south polar caps, *J. Geophys. Res., 76,* 4262, 1971.

Williams, D. J., and C. O. Bostrom, Proton entry into the magnetosphere on May 26, 1967, *J. Geophys. Res., 74,* 3019, 1969.

Williams, D. J., and G. D. Mead, Nightside magnetosphere configuration as obtained from trapped electrons at 1100 kilometers, *J. Geophys. Res., 70,* 3017, 1965.

(Received February 16, 1972;
accepted April 26, 1972.)